Journal of Hydrology 613 (2022) 128460

Contents lists available at ScienceDirect

Journal of Hydrology

journal homepage: www.elsevier.com/locate/jhydrol

Research papers

Changes in soil moisture caused solely by vegetation restoration in the karst region of southwest China

Dawei Peng [a], Qiuwen Zhou [a,*], Xin Tang [b], Weihong Yan [a], Meng Chen [a]

[a] School of Geography and Environmental Science, Guizhou Normal University, 550001 Guiyang, People's Republic of China
[b] The Third Surveying and Mapping Institute of Guizhou Province, 550004 Guiyang, People's Republic of China

ARTICLE INFO

Keywords:
Soil moisture
Vegetation
Karst
southwest China
Random forest
Rocky desertification
Ecological engineering
Vegetation greening
Climate change

ABSTRACT

Large-scale vegetation restoration projects have been ongoing in the karst region of southwest China for several years. However, the influence of vegetation restoration alone on soil moisture (SM) changes in this region remains unclear. In this study, a random forest model was constructed using meteorological data, the ERA5-Land SM dataset, and the enhanced vegetation index to analyze SM changes in the karst region of southwest China caused by vegetation restoration alone. The results showed that on a monthly scale, vegetation restoration introduced an increase in SM that was mainly concentrated in January–April and a decrease that was mainly concentrated in June–August. On a seasonal scale, vegetation changes caused an increase in mean SM in spring and winter and a decrease in mean SM in summer and autumn. The largest increase in SM owing to vegetation changes was in spring, with an average increase of 0.019 m^3/m^3, and the largest decrease was in summer, with an average decrease of 0.010 m^3/m^3. However, the annual average SM increased only slightly. On the seasonal and annual scales, the coefficient of variation values for changes in SM caused by vegetation restoration alone were dominated by decreases, with a large decrease from January to April. In addition, vegetation restoration effectively moderated the drying tendency of soil caused by climate warming.

1. Introduction

Soil moisture (SM) is an important component of the soil–plant–atmosphere hydrological continuum that affects the stability of ecosystems via regulating the growth and development of vegetation (Heathman et al., 2003; Legates et al., 2011; Wang et al., 2018; Yu et al., 2018; Yu et al., 2020; Zhang et al., 2021). Climatic factors have a great influence on SM over long periods of time and on a large scale. In addition, the effect of changes in vegetation on SM cannot be neglected. This is especially true for regions in which vegetation has considerably changed in recent years owing to human activity (Mittelbach and Seneviratne, 2012; Niether et al., 2017). Therefore, exploring the impact of vegetation restoration on SM (including its content and stability) is an important issue that must be resolved to understand maintenance of ecosystem stability.

Studies that have analyzed the impact of vegetation changes on SM can be categorized as global or regional studies (Feng and Liu, 2015; Gu et al., 2019). The impact of changes in vegetation on SM at the global scale is usually small because large vegetated areas have not considerably varied at the global scale (Feng, 2016). Regionally, some case studies have been conducted in certain areas with substantial vegetation changes. Studies in semiarid and subhumid areas have shown that vegetation restoration causes a decrease in SM (Bellot et al., 2004; Yang et al., 2014; Cao et al., 2018; Liang et al., 2018; Liu et al., 2018; Zhang and Shangguan, 2016; Zhang et al., 2016; Zhang et al., 2020). However, vegetation restoration in humid areas has varying impacts on SM under different environmental conditions (Adams et al., 1991; Van Hall et al., 2017; Hiltbrunner et al., 2012). The situation in humid regions is complicated, because under sufficient precipitation, factors such as water depletion by vegetation, soil, and bedrock water storage capacity affect the relationship between vegetation changes and SM (Zhang et al., 2014; Cámara et al., 2017; Li et al., 2017).

Humid karst areas are humid climate areas with shallow soil layers and bedrock that is highly permeable to water (Hartmann et al., 2014; Deng et al., 2020). These characteristics are likely to result in a different SM response caused by vegetation restoration compared with other humid areas. Studies in humid karst areas mainly include case studies conducted on sample sites and regional studies based on remote sensing or reanalysis data. In the former, few sample plots are usually selected to study the effect of vegetation changes on SM under specific

* Corresponding author.
E-mail address: zouqiuwen@163.com (Q. Zhou).

https://doi.org/10.1016/j.jhydrol.2022.128460
Received 12 June 2022; Received in revised form 23 August 2022; Accepted 1 September 2022
Available online 20 September 2022

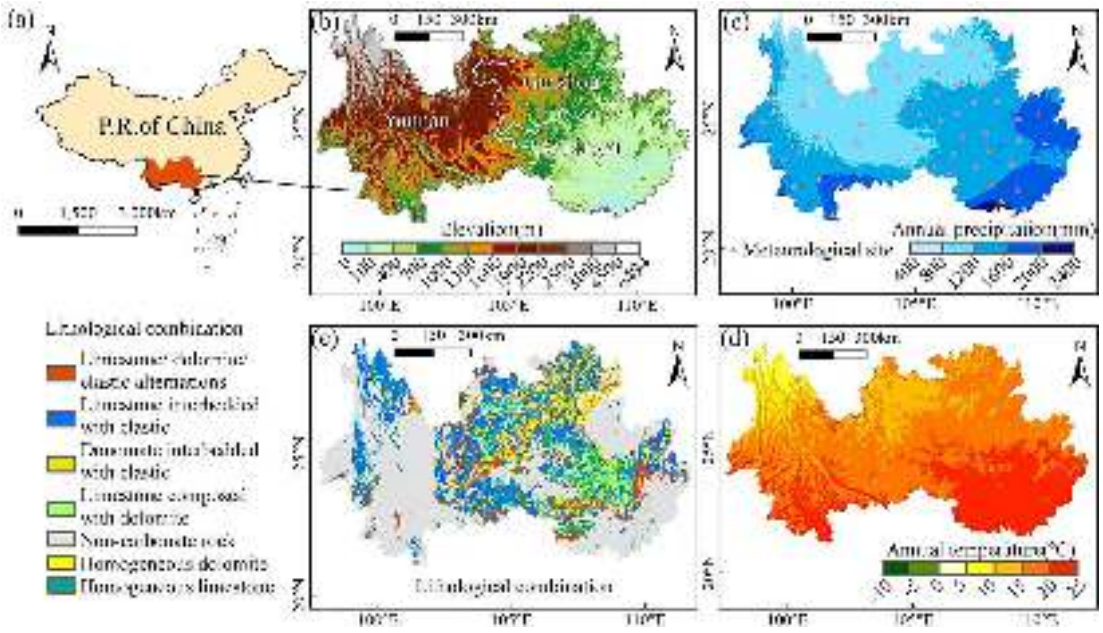

Fig. 1. The location (a), elevation (b), precipitation (c), temperature (d), and lithology (e) of the study area. The white lines in (b) indicate provincial boundaries.

environmental conditions (Fu et al., 2016; Zhou et al., 2022). However, mountainous karst regions have high environmental heterogeneity that a few case studies are not sufficient to illustrate the overall effect in humid karst areas. Specifically, lithology, soil thickness, topography, and vegetation growth conditions can considerably vary in different karst mountain regions, and these factors can affect the relationship between vegetation changes and SM (Yan et al., 2021; Yan et al., 2022). In contrast, regional-scale studies based on remote sensing or data reanalysis are better able to reflect general patterns in humid karst regions. However, these previous regional-scale studies only analyzed SM trends and did not exclude the influence of climate so as to separately assess the changes in that result from vegetation restoration alone (Deng et al., 2020). Therefore, changes in SM due to solely vegetation restoration in humid karst areas remains unclear.

In areas with significant vegetation restoration, failing to consider SM changes influenced solely by vegetation restoration may lead to inaccurate understanding of the effects of vegetation restoration on SM. If vegetation restoration and climate change lead to SM changes in opposite directions, their combined effect will result in smaller SM changes, and the effects of climate change and vegetation restoration on SM may be underestimated. Specifically assessing SM changes influenced by vegetation restoration alone can thus help accurately understand whether vegetation restoration enhances or slows down SM changes caused by climatic factors.

The relationship between vegetation change and SM change in karst areas in humid regions is complex, and vegetation restoration in humid karst areas has been obvious in recent years (Zhang et al., 2019; Zhong et al., 2022). As mentioned earlier, studies conducted in humid karst areas have not excluded the influence of climate change on vegetation restoration in such areas. Therefore, SM changes caused by vegetation restoration alone in humid karst areas as well as whether vegetation restoration mitigates or exacerbates soil moisture changes caused by climatic factors remain unclear.

Given that increased vegetation consumes more water, we hypothesized that vegetation restoration alone in the karst region of southwest China would result in obvious changes in SM. The aim of this study was to confirm whether and to what extent SM content and its stability have changed. In this study, the coefficient of variation of SM was used to characterize the stability of SM. By constructing a random forest model (RFM) using SM data from 2001 to 2003, we simulated SM content affected by vegetation restoration alone from 2004 to 2019. To assess changes in soil moisture content and coefficient of variation caused due to vegetation restoration alone, the simulated results were compared with SM data collected before vegetation restoration (2001).

2. Materials and methods

2.1. Study area

The study areas in this work were in Yunnan Province, Guizhou Province, and the Guangxi Autonomous Region in southwestern China, which accounted for approximately 796,773 km^2 (Fig. 1a). The elevation of the area increases from southeast to northwest (Fig. 1b). The terrain is dominated by plateaus and mountains. The climate is mainly subtropical humid monsoon climate. The average annual precipitation is approximately 1021 mm (Fig. 1c) and the annual average temperature is approximately 17.6 °C (Fig. 1c, d). The geology of this area is complex, with a large area of carbonate rocks, mainly consisting of limestone and dolomite (Fig. 1e). The soil in the area is mainly haplic alisols (common topsoil fractions: 40 % sand, 37 % silt, and 23 % clay), chromic luvisols (topsoil fractions 27 % sand, 27 % silt, and 46 % clay), rendzic leptosols (topsoil fractions: 37 % sand, 44 % silt, and 19 % clay), and dystric regosols (topsoil fractions: 42 % sand, 37 % silt, and 21 % clay). The soil is loose and erodible and forms a thin layer. The vegetation types in the area are diverse, although areas of carbonate rock area mainly suitable for the growth of shrubs and grasses, whereas areas of noncarbonate rock can support arbor forests. The unique geological conditions in this area, which have led to extensive development of karst landforms, is the most typical karst landform in eastern Asia. The formation of karst landforms has caused severe soil erosion and water shortages, which are not conducive to the development of agricultural production, transportation, and urbanization, resulting in limited social and economic development. Vegetation in this region has been extensively damaged by reclamation of sloping land, grazing, and firewood cutting before the 1990s. Since around 2000, various large-scale ecological projects were initiated to restore the ecology of the area. The main ecological engineering measures taken here are to reduce human interference, thereby achieving secondary vegetation succession. Although additional measures, such as afforestation, have been implemented in certain places, the area covered by these actions is limited.

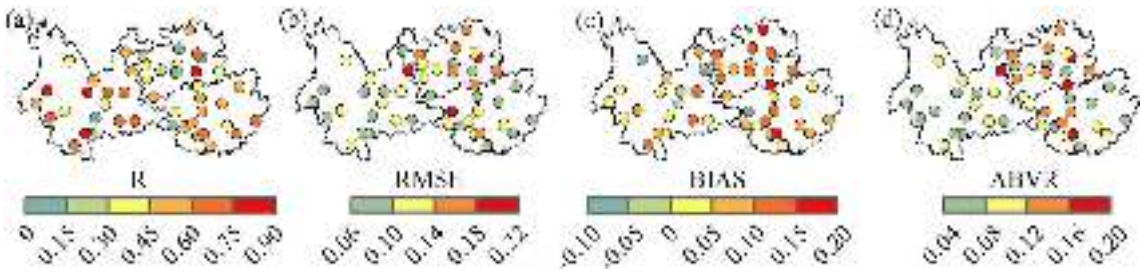

Fig. 2. Correlation coefficient (a), RMSE (b), BIAS (c), and ABVR (d) between the ERA5-Land and measured data of various field observation sites.

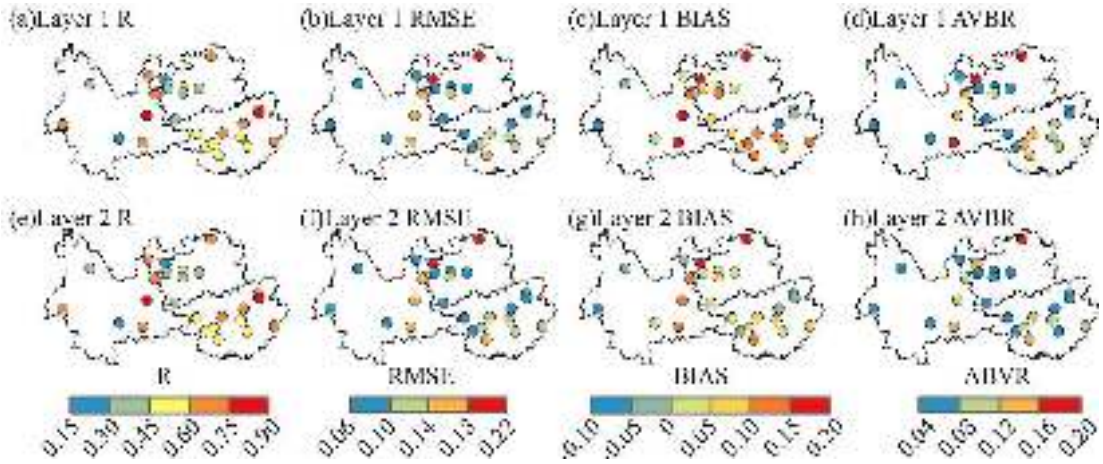

Fig. 3. Correlation coefficient (a), RMSE (b), BIAS (c), and ABVR (d) between the gravimetric-based and ERA5-Land SM datasets.

2.2. Data source and processing

2.2.1. SM data

SM data for the entire study area were obtained in raster format from the global ERA5-Land SM dataset (https://cds.climate.copernicus.eu/). Compared with the more commonly used types of remote sensing or reanalysis SM data, ERA5-Land has a higher spatial resolution and can better detect spatial variations in SM within the highly heterogeneous karst environment. Although SM products such as those from the Soil Moisture Active and Passive satellite have high spatial resolution, it only represents SM to a depth of 0–5 cm in the soil layer, whereas ERA5-Land detects SM variations in deeper soil levels (root zone). Therefore, ERA5-Land data were used in this study. The ERA5-Land SM data consists of four vertical layers (0–7, 7–28, 28–100, and 100–289 cm). Since the study was conducted in a humid karst area with shallow soil layers, only SM data within a 100-cm depth were selected. The spatial resolution of the data was 0.1° × 0.1°, the time resolution was daily, and the time range was 2000–2019. After preprocessing the SM data to remove erroneous values, the average value and coefficient of variation (CV) of the study area in the spring, summer, autumn, winter, active growing season (AGS), and each month were calculated for analysis.

The field-measured SM dataset in this article was obtained from the Chinese Crop Growth and Farmland Soil Moisture Dataset compiled by the China National Meteorological Science Data Center (https://data.cma.cn/). The sampling depth of the dataset was 0–10 cm, the time resolution was 10 days, and the time range was 2000–2013. After removing sites lacking data, 44 sites in the study area were selected. Since the measured SM data at the sites were the relative moisture content, the relative SM content was multiplied by the field water holding capacity and the soil bulk density to obtain the soil volumetric moisture content. Owing to the lack of data on field water holding capacity and soil bulk density at each site, the values of these two parameters were obtained from studies. Since the data were measured in farmland, it is anthropogenic soil, the soil bulk density is 1.37 g/cm^3 (Albergel et al.,2012), and the field water holding capacity was set at 30 % (Brocca et al., 2010). The accuracy of all ERA5-Land SM dataset was verified by converting the relative soil humidity to soil volumetric water content. Since the available field-measured SM data were recorded on a 10-day scale, the accuracy of the ERA5-Land SM dataset of the study area could only be verified on a 10-day scale.

Given that the previous SM field observation dataset was limited to surface data, a China-wide gravimetric-based multilayer SM dataset was used for further validation (Wang and Shi, 2019). This dataset included month-wise data of soil depths of 0–10 cm, 10–20 cm, 40–50 cm, 60–70 cm, and 90–100 cm from 1992 to 2013. To match the soil layers of the ERA5-Land SM data, we used the 0–10-cm and 10–20-cm data from the gravimetric-based dataset to match with the 0–7-cm and 7–28-cm SM data from the ERA5-Land dataset. We did not validate the 28–100-cm SM data from ERA5-Land due to multiple layers of missing data at 40–100 cm depth in the gravimetric-based multilayer SM dataset.

2.2.2. Enhanced vegetation index and meteorological data

The enhanced vegetation index (EVI) data (MOD13A3) were obtained from the National Aeronautics and Space Administration (http://reverb.echo.nasa.gov/reverb/). The spatial resolution of the MOD13A3 dataset was 1 km, the time resolution was monthly, and the time range was 2000–2019. After preprocessing the data, such as removal of spatial mosaics and erroneous values, linear interpolation was performed pixel-by-pixel in time. The higher temporal resolution of EVI means that it is more likely to be affected by cloud cover occlusion, anomalies, and other factors, thereby leading to larger errors; therefore, this paper uses the maximum synthetic monthly scale data, so that the EVI more truly reflects the vegetation conditions in the study area. After linear interpolation, the data time resolution was daily. After spatial resampling of the data, the spatial resolution was 0.1° × 0.1°.

The temperature and precipitation data (China Surface

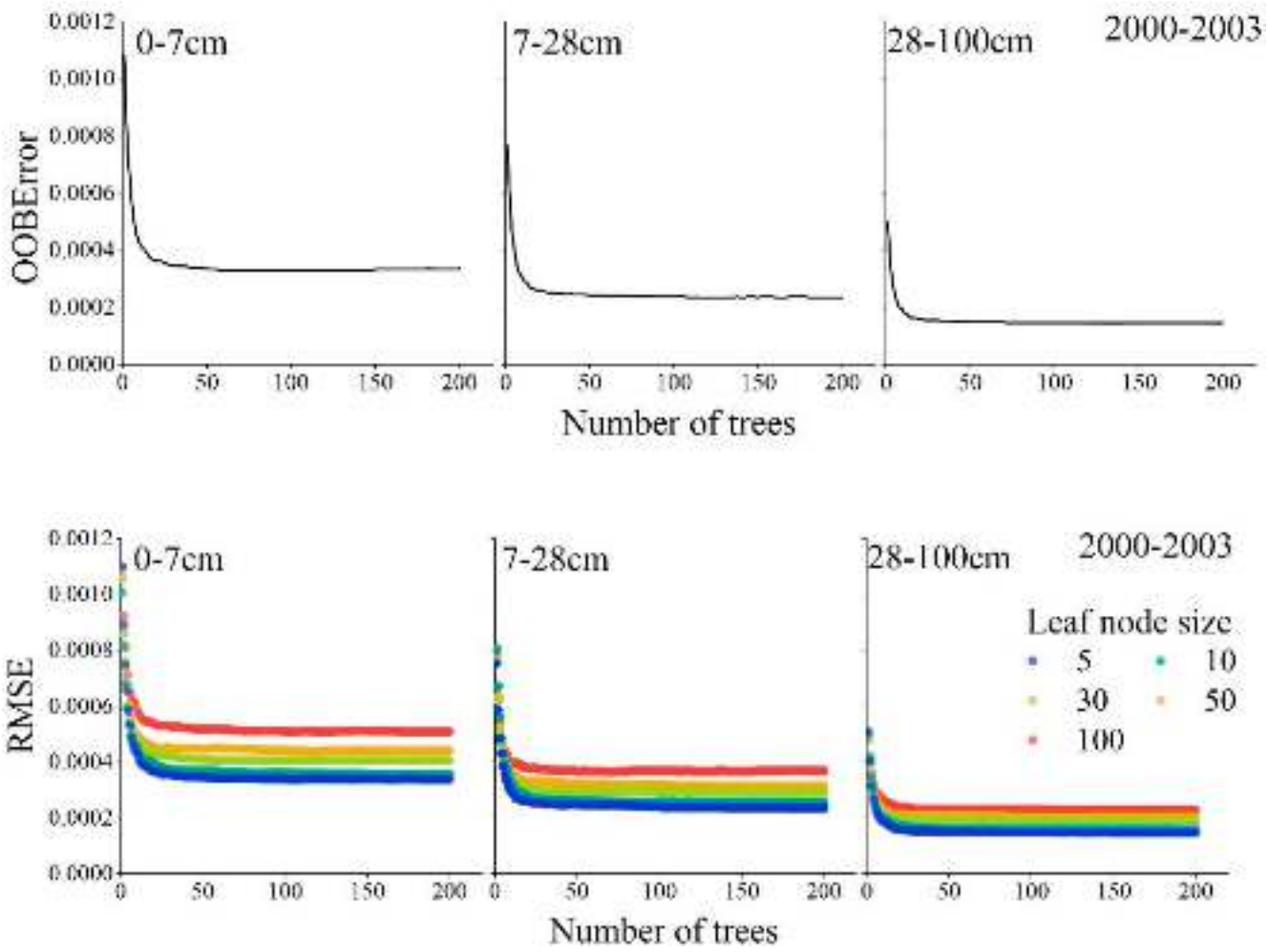

Fig. 4. Optimal number of trees and minimum leaf node parameter selection for the random forest model for 2000–2003.

Meteorological Daily Value Dataset V3.0) were obtained from the China National Meteorological Science Data Center (http://data.cma.cn/). The time resolution of the dataset was daily and the time range was 2000–2019. After preprocessing the original data, Anusplin software (https://fennerschool.anu.edu.au/research/products/anusplin) was used to perform day-to-day spatial interpolation. The spatial resolution of the data after interpolation was 0.1° × 0.1°.

2.3. Methods

2.3.1. RFM

A RFM was used to analyze the impact of vegetation on SM. The RFM was an ensemble learning algorithm based on a decision tree. The algorithm can be roughly divided into a classification algorithm and a regression algorithm. In this study, the regression algorithm was used. The regression algorithm is based on a combined model composed of a set of regression decision subtrees $\{h(x,\theta_t),t = 1,2,\ldots,T\}$, where θt is a random variable subject to independent and identical distribution, x is the independent variable, and T is the number of decision trees. Ensemble learning uses the value of each decision tree $\{h(x,\theta_t)\}$ as the regression prediction result as described in Eq. (1):

$$\overline{h}(x) = \frac{1}{T}\sum_{t=1}^{T}\{h(x,\theta_t)\} \quad (1)$$

where $h(x,\theta_t)$ is the output based on × and θ. The RFM generates different decision trees from different subsets of training data through the bagging process, thereby avoiding the effects of multicollinearity between independent variables (Breiman, 2001; Segal and Xiao, 2011).

To date, RFMs have been applied in many ecohydrological studies and their reliability in ecohydrology has been verified by multiple groups (Carranza et al., 2021; Zhang et al., 2021). Because the onset of large-scale vegetation restoration in the karst region of southwest China was around 2000, and no clear effects were observed during the initial years, the data from 2000 to 2003 were used to establish the RFM and data from 2004 were used for verification. The regression algorithm is summarized as the formula in Eq. (2):

$$SM = aP + bT + cEVI = dP_p + eT_p + f \quad (2)$$

where a to e are regression parameters, f is a constant, and the independent variables P, T, EVI, T_p, and P_p are the daily precipitation, temperature, EVI, previous temperature, and previous precipitation from 2000 to 2003, respectively, and the dependent variable SM is the daily SM from 2000 to 2003. As the hydrological process in the karst area is relatively rapid (Fu et al., 2015; Huang et al., 2009), the temperature and precipitation data over the preceding three days were used as the previous meteorological elements.

After constructing the model, we substituted the independent variable from 2004 into the model and compared the simulated SM values with those from ERA5-Land to verify the reliability of the model. 2001 was chosen as the base period because a large-scale vegetation restoration project was implemented around 2000, and EVI data for a whole year are available for 2001, which represents the period before vegetation changes. We chose 2019 as the period of change, which represents

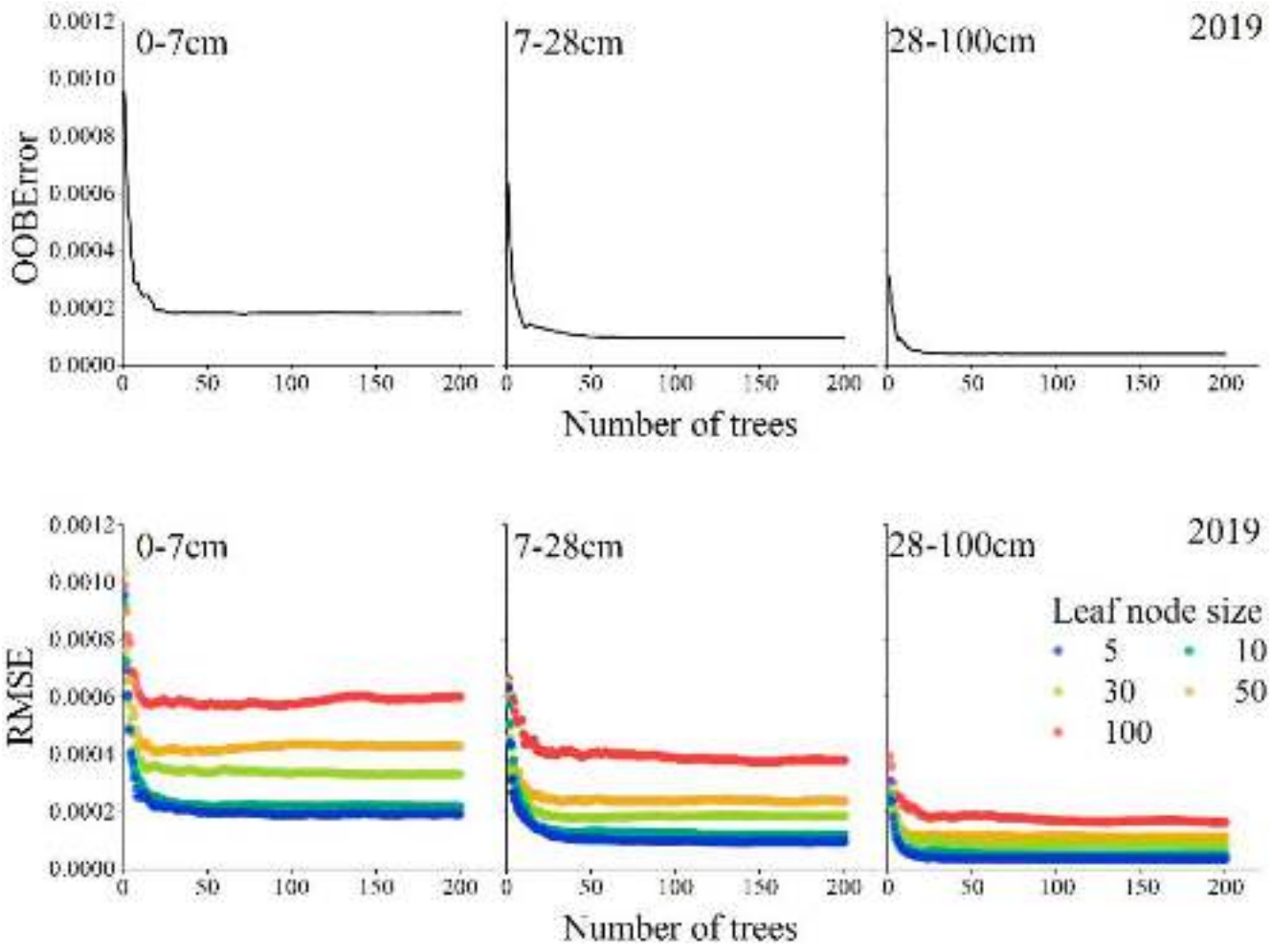

Fig. 5. Optimal number of trees and minimum leaf node parameter selection for the random forest model in 2019.

the time after vegetation restoration. Although vegetation changes did occur to a small degree in the first few years after the vegetation restoration was implemented, we used only data from 2001 rather than the average from 2001 to 2003 to optimally represent conditions before vegetation restoration. We substituted the daily precipitation, daily temperature, previous precipitation, and previous temperature from 2001, along with the EVI for 2019 into the model, thus simulating the effect SM from vegetation change alone.

2.3.2. Methods for determining SM under different influencing factors

After obtaining the daily SM data under the condition that the vegetation did not change in 2019 through the RFM, the change in the mean value and CV of SM caused by the vegetation change alone were calculated according to Eq. (3) and (4):

$$SM_{v-mean} = SM_{2019-mean} - SM_{p-mean} \quad (3)$$

$$SM_{v-cv} = SM_{2019-cv} - SM_{p-cv} \quad (4)$$

where $SM_{2019\text{-}mean}$ and $SM_{2019\text{-}cv}$ are the mean value and CV of the SM after vegetation change, respectively, which was obtained via substituting the daily precipitation, daily temperature, previous precipitation, and previous temperature from 2001, as well as the EVI for 2019 into the RFM model. $SM_{p\text{-}mean}$ and $SM_{p\text{-}cv}$ are the mean value and CV of the SM before vegetation change, and here we used the ERA5-Land data from 2001 (base period) to represent SM before vegetation changes. $SM_{v\text{-}mean}$ and $SM_{v\text{-}cv}$ are the changes in the mean value and CV of SM before and after vegetation restoration caused only by vegetation restoration. A positive value for $SM_{v\text{-}mean}$ indicates that vegetation restoration increased the mean value of SM content, while a negative value indicates that vegetation restoration decreased the mean value of SM content. The $SM_{v\text{-}cv}$ value was calculated similarly.

The difference between the changes in SM caused by vegetation alone and those caused by comprehensive factors, including climate, vegetation restoration, and other unspecified factors, were calculated using Eq. (5) and Eq. (6):

$$C_{mean} = SM_{y-mean} - SM_{c-mean} \quad (5)$$

$$C_{cv} = SM_{v-cv} - SM_{c-cv} \quad (6)$$

where C_{mean} is the difference between SM changes caused by vegetation restoration alone and those caused by comprehensive factors. Accordingly, C_{cv} is the difference between the CV of SM changes caused by vegetation restoration alone and those caused by comprehensive factors. A positive value of C_{mean} indicates that the change to the average SM content caused by vegetation restoration alone is higher than that caused by comprehensive factors, whereas a negative value of C_{mean} indicates the opposite and C_{cv} is similar. $SM_{c\text{-}mean}$ and $SM_{c\text{-}cv}$ are the mean value and CV of the SM change before and after vegetation restoration under the influence of comprehensive factors. $SM_{c\text{-}mean}$ was obtained by subtracting the actual SM value for 2001 from the actual SM for 2019 from the ERA5-Land data. $SM_{c\text{-}cv}$ was obtained in a similar way.

The above calculations were performed on three different time scales: monthly, seasonally, and yearly. Moreover, the significance of all comparisons was tested. Since the data were not normally distributed,

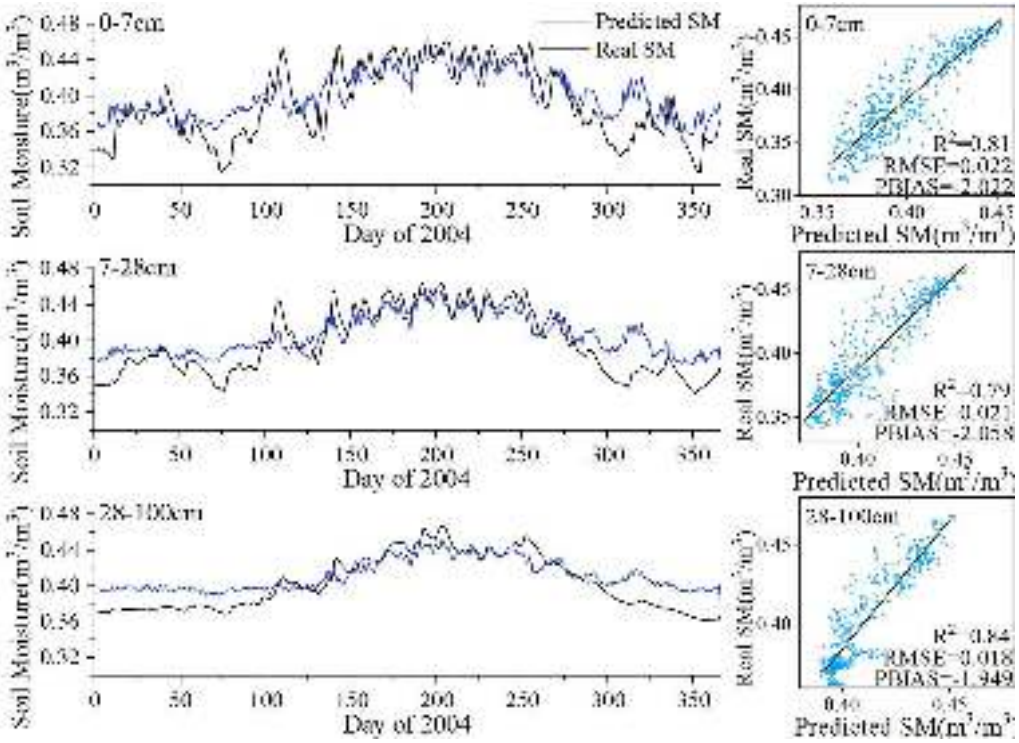

Fig. 6. Comparison of the predicted SM data from the RFM model with the ERA5-Land SM data.

the Kruskal–Wallis test was used for analysis.

3. Results

3.1. Accuracy validation and model parameter determination

Field-measured SM data from 2000 to 2013 were used to verify the ERA5-Land SM dataset. On a 10-day scale, the ERA5-Land SM dataset overestimated the actual SM values. The correlation coefficient between the ERA5-Land SM dataset and field-measured SM data was >0.3 for 82.61 % of the sites and >0.5 for 50 % of the sites (Fig. 2a), whereas the root-mean-square error (RMSE) was <0.1 for 45.45 % of the sites (Fig. 2b), the BIAS between value was ±0.1 for 77.27 % of the sites (Fig. 2c), and the ABVR was <0.12 for 43.48 % of the sites (Fig. 2d). The sites were evenly distributed in space, indicating that ERA5-Land SM data of the karst region in southwest China were highly accurate and sufficient for this study.

The gravimetric-based SM dataset also showed that ERA5-Land slightly overestimates actual SM. The average correlation coefficient between ERA5-Land and the measured SM in the first layer was 0.55, and 44 % of the sites had a correlation coefficient greater than 0.6, while the second layer had an average correlation coefficient of 0.48, and 28 % of the sites had a correlation coefficient greater than 0.6 (Fig. 3a, e). The average RMSE of ERA5-Land and the measured SM in the first layer was 0.10, and 52 % of the sites had an RMSE less than 0.1, while the second layer had an average RMSE of 0.09, and 68 % of the sites had an RMSE less than 0.1 (Fig. 3b, f). The average BIAS of ERA5-Land and the measured SM in the first layer was 0.07, and 56 % of the sites had a BIAS between ±0.1, while the second layer had an average BIAS of 0.05, and 76 % of the sites had a BIAS between ±0.1 (Fig. 3c, g). The average AVBR of RA5-Land and the measured SM in the first layer was 0.09, and 52 % of the sites had an AVBR less than 0.08, while the second layer had an average AVBR of 0.08, and 60 % of the sites had an AVBR less than 0.08 (Fig. 3d, h).

For 2000–2003 and 2019, when the number of trees in the RFM was 50–100, the OOBError of all soil layers tended to be stable and the RMSE of all soil layers reached a minimum when the number of leaf nodes was five (Figs. 4 and 5). Considering the high heterogeneity of the karst mountain environment, more trees may need to be built in the local area to stabilize the OOBError of the model. Thus, we herein used 100 trees for pixel-by-pixel modeling.

The 2004 dataset was used to verify the prediction results of the RFM model. Overall, the RFM model has high prediction accuracy, with an average R^2 of approximately 0.8, an average RMSE of 0.02, and an average PBIAS of 2.0 % (Fig. 6). From the perspective of different seasons, the data predicted using the RFM model demonstrated high accuracy during the growing season. However, there was some difference between the predicted value and the ERA5-Land SM data during the nongrowing season.

3.2. Temporal and spatial changes in vegetation and SM content

The vegetation change from 2000 to 2019 was dominated by a substantial upward trend, accounting for approximately 86.99 % of the study area (Fig. 7a, b, c, i). Only a few areas showed a decreasing trend in EVI, which were mainly distributed in the western part of the study area (Fig. 7l). However, SM content remained generally stable, with only a slight increase in SM content in the lower layers. (Fig. 7a, b, c). The pixel-by-pixel correlation analysis showed that despite the weak overall correlation between EVI and SM content, some local areas with high correlation were still identified (Fig. 7d). In addition, the areas with low SM and EVI were mainly distributed in the northwest part of the study area, while areas with high SM and EVI are mainly found in the northeast part of the study area (Fig. 7e, f, g, h).

The rates at which vegetation and climate contribute to SM content changes from 2000 to 2019 are shown in Fig. 8. The contribution of climatic factors to SM variation was 61.8 %, whereas the contribution of vegetation factors was 38.2 %. However, this feature varies from month to month. The contribution rate of climatic factors to SM content changes in autumn and winter was considerably higher than that of vegetation restoration, whereas the opposite was true in summer. Among the summer months, the contribution of climatic factors at

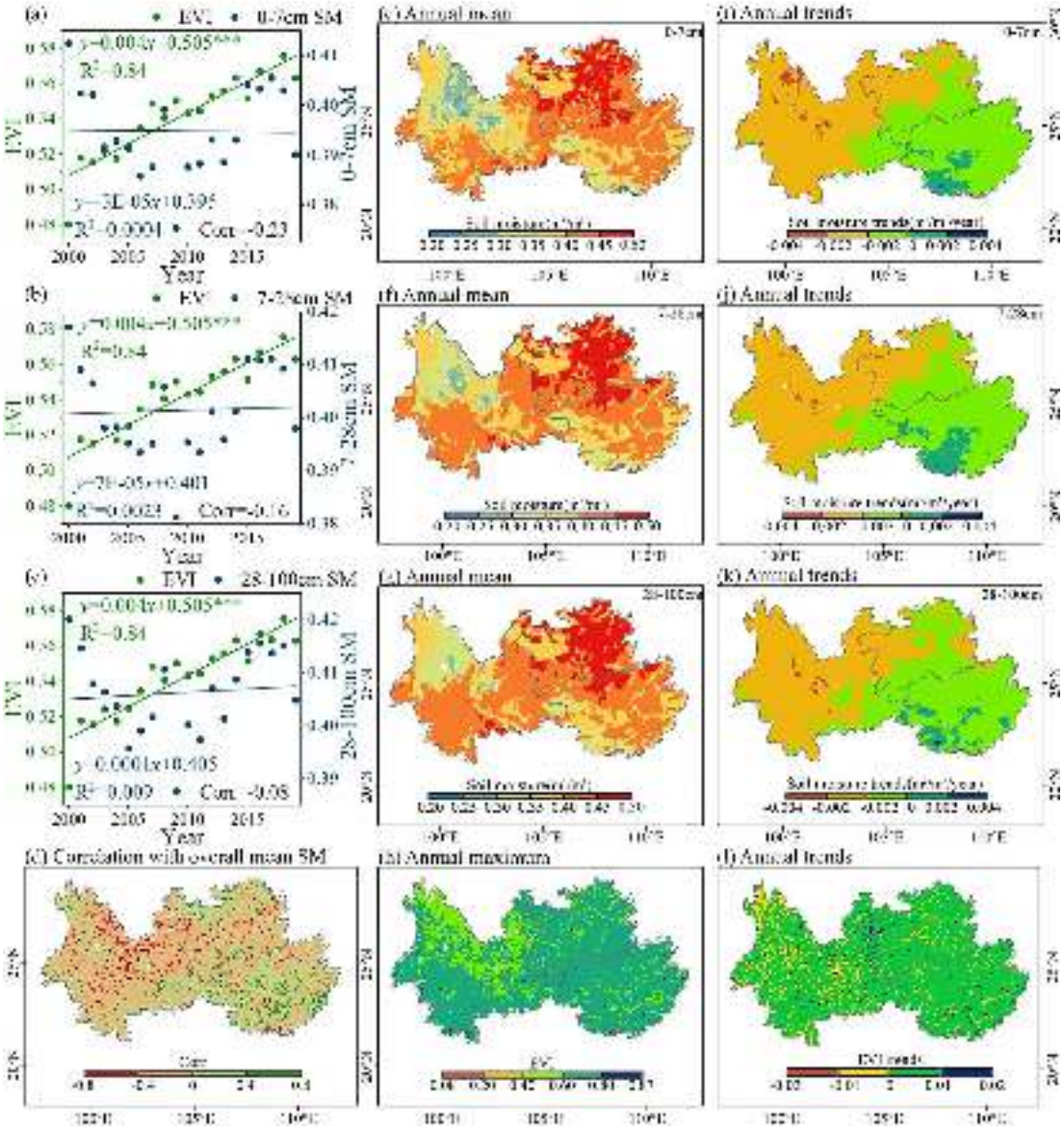

Fig. 7. Trends in EVI and SM at different depths (a, b, c). Light green indicates EVI, dark green indicates SM, *** indicates that a trend passed the significance test at the 0.001 level. Correlation of EVI and SM on a pixel-by-pixel scale (d). The spatial distribution of SM (e, f, g) and the spatial distribution of trends in SM variation at different depths (i, j, k). The spatial distribution of trends in the annual maximum EVI (h) and EVI (l).

depths of 0–7 and 7–28 cm in September exceeded 95 %. There were also differences in the contribution rates of climate and vegetation change factors at different soil layer depths in spring. The climate and human activity factors contributed to SM content changes at similar rates in the 0–7 cm soil layer, as well as in the deeper soil layers. However, vegetation restoration contributed more.

3.3. Response of the average SM to vegetation changes alone

On a monthly scale, vegetation changes alone lead to an increase in mean SM in the first half of the year and a decrease in mean SM in the second half of the year. This increase in SM was mainly concentrated in January–April while the decrease was mainly concentrated in June-–August. The average SM decreased with increasing soil depth owing to vegetation change. (Fig. 9). The SM content in the 0–7-cm soil layer increased the most from January to April, with an average increase of 0.031 m^3/m^3, whereas the SM content decreased the least from June to August, with an average decrease of 0.008 m^3/m^3. In the 28–100-cm soil layer, the increase in SM content was the smallest from January to April, with an average increase of 0.018 m^3/m^3, whereas the decrease in SM content was the largest from June to August, with an average decrease of 0.013 m^3/m^3 (Fig. 9).

On a seasonal scale, vegetation changes led to an increase in mean SM in spring and winter, a decrease in mean SM in summer and autumn, and a minor change in mean SM in AGS. The largest increase in SM content owing to vegetation change occurred in spring, with an average increase of 0.019 m^3/m^3, and the largest decrease occurred in summer, with an average decrease of 0.010 m^3/m^3. With greater soil depth, the rise in SM rise gradually decreased during the spring and the decline in SM gradually increased during the summer (Fig. 10). The increase in SM in spring decreased from 0.022 m^3/m^3 to 0.017 m^3/m^3, whereas the decrease in SM in summer increased from 0.008 m^3/m^3 to 0.0013 m^3/m^3 (Fig. 10).

Overall, vegetation restoration induced a slight increase in the annual average SM, whereas the SM content in summer remained stable (Fig. 11a). Since 2004, the average annual SM caused by vegetation restoration has increased from 0.0007 m3/m3 to 0.0060 m^3/m^3, with an average annual increase of 0.0004 m^3/m^3. The overall SM in summer

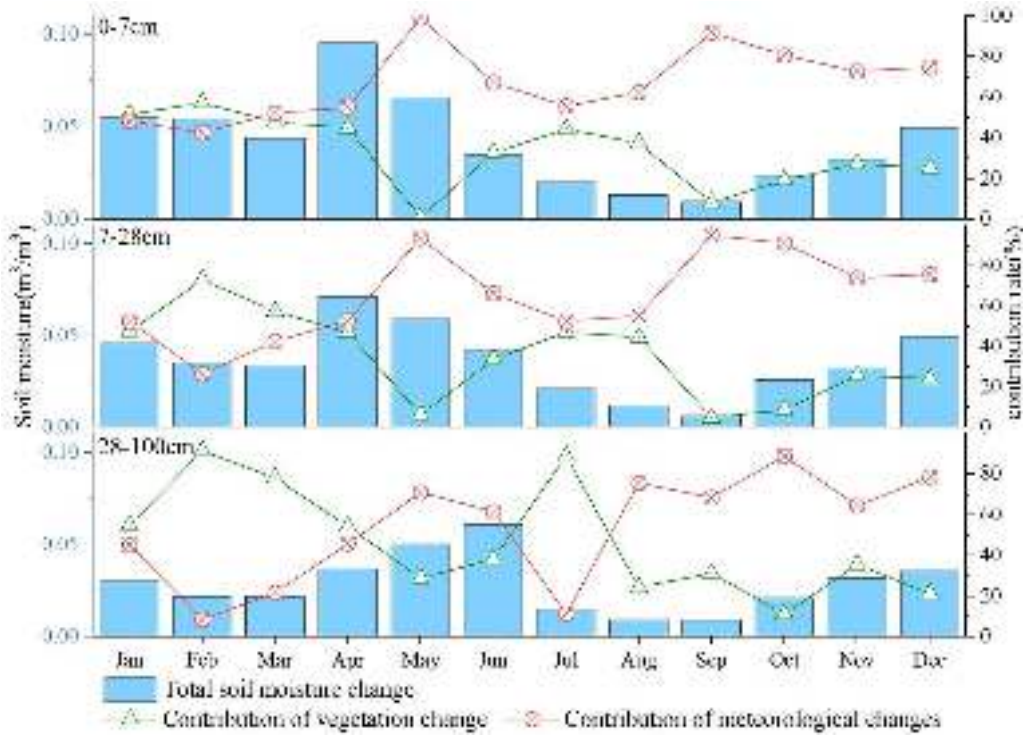

Fig. 8. Contribution rates of climate and vegetation factors to SM content changes on a monthly scale.

has shown a slight downward trend with an average annual rate of 0.0001 m^3/m^3. This feature also displayed evident differences among different regions (Fig. 11b, c, d). Areas that experienced an increase in annual average SM accounted for 54.85 % of the total study area and were mainly located in the western part of the study area, whereas areas that underwent a decrease in annual average SM were mainly in the eastern part of the study area. At greater soil depths, there are larger areas of increased annual average SM. In the 28–100-cm soil layer, the area with increased SM due to vegetation changes increased to 55.13 % of the total area (Fig. 11d).

From a comparison of average SM changes caused by vegetation restoration alone and those owing to comprehensive factors (including climate, vegetation restoration, and other unspecified factors), the former was greater than the latter in most months, and only in January and July was the former smaller than the latter. On the seasonal scale, all seasons displayed greater changes in average SM owing to vegetation restoration alone than those owing to the comprehensive factors (Fig. 12).

3.4. Response of SM CV to vegetation change alone

At the monthly scale, vegetation restoration alone mainly led to a decrease in the CV of SM, with a generally larger decrease from January to April, resulting in an average decrease in SM CV of 0.077. Vegetation restoration led to an increase in the CV of SM for June–July, resulting in an average increase in SM CV of 0.011. The decrease in CV of SM decreased gradually with increasing soil depth in most months, and the decrease in CV of SM gradually increased in May only, its decrease increased from 0.027 to 0.043 (Fig. 13).

On the seasonal scale, the changes in CV of SM caused by vegetation restoration alone were dominated by decreases, with the largest decrease in spring, resulting in an average decrease in soil moisture CV of 0.080. Only summer experienced a slight increase in the CV of SM, on average The decrease in CV of SM caused by vegetation restoration alone gradually decreased with increasing soil depth in spring, winter, and AGS. 0.021 and 0.018 (Fig. 14).

At the annual scale, vegetation restoration alone reduced the CV of SM across most of the study area. The area with reduced CV accounted for 98.27 % of the total study area on average, with the main source of the reduction occurring in the northwestern part of the study area. The reduction in CV of SM owing to vegetation restoration alone decreased with increasing soil depth (Fig. 15).

A comparison of the variation in CV of SM caused by vegetation restoration alone and that caused by comprehensive factors (climate, vegetation restoration, and other unspecified factors) reveals that the former was lower than the latter in most months, and was higher than the latter only in July. On the seasonal scale, the variation in CV of SM due to vegetation restoration alone was lower than that due to the comprehensive factors in all seasons (Fig. 16).

4. Discussion

4.1. Time variations in SM changes due to vegetation restoration alone

The results of this study demonstrate that vegetation restoration in a subtropical humid karst area resulted in a slight increase in annual average SM content (Fig. 11). However, existing plot-scale case studies in humid karst areas have previously found that vegetation restoration resulted in a slight decrease in SM content (Zhou et al., 2022). These results collectively indicate that vegetation restoration in subtropical humid karst regions has little effect on overall SM content. On the one hand, vegetation restoration causes an increase in vegetation cover, which leads to lower soil evaporation (Li et al., 2019). Additionally, vegetation restoration leads to the formation of a thicker litter layer, and the more extensive root system and greater organic matter help form a good aggregate structure in the soil, which will increase the water holding capacity of the soil (Yang et al., 2016; Yang et al., 2017; Zhang et al., 2019). The above changes are beneficial for increasing SM content in karst areas, which are typically characterized by massive water seepage. However, the increase in transpiration brought about by vegetation restoration cannot be ignored (Ning et al., 2020; Wang et al., 2022), especially in subtropical regions. Vegetation restoration in

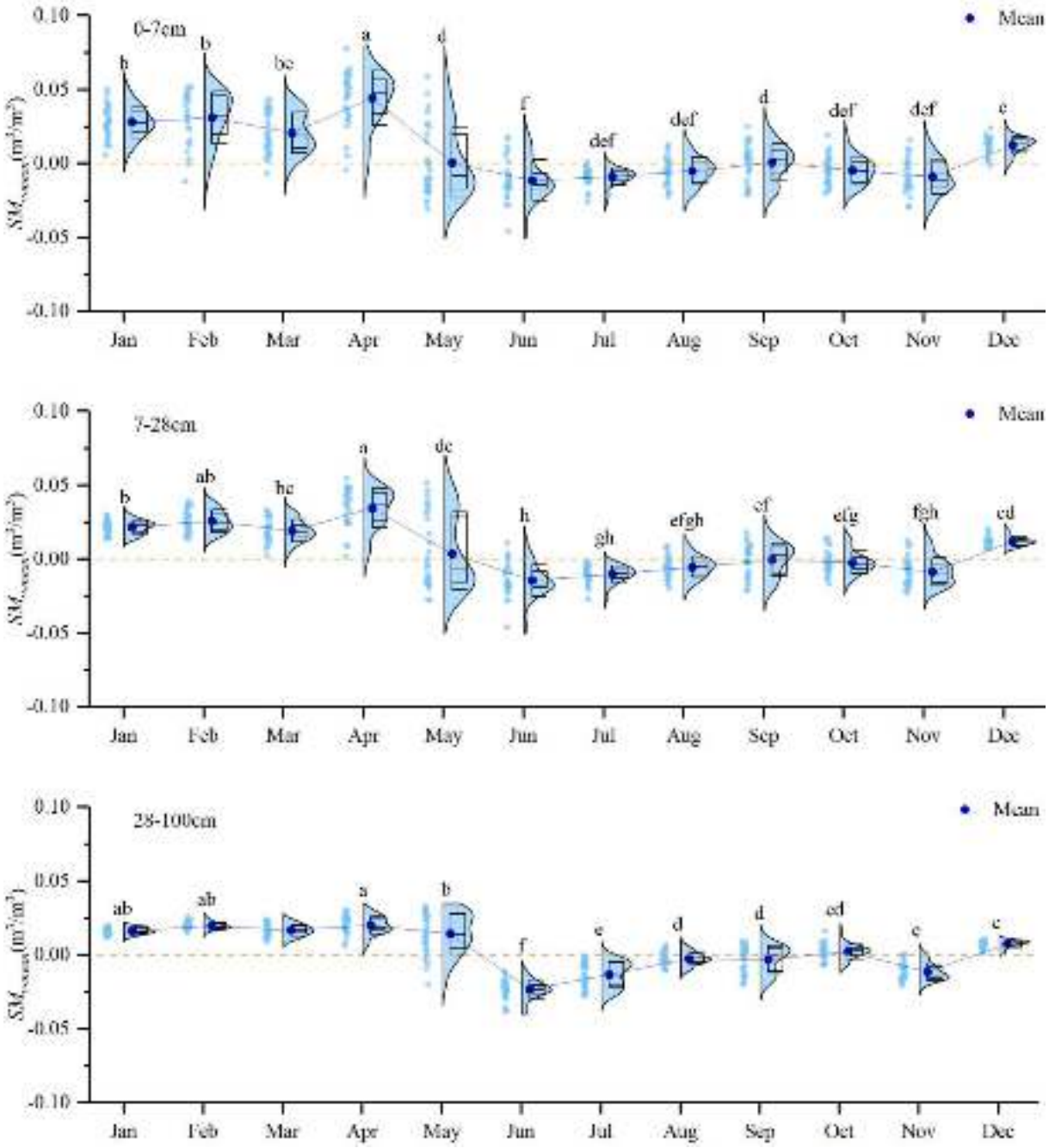

Fig. 9. Monthly changes to average SM in different soil layers caused by vegetation restoration alone in the karst region of southwest China.

subtropical humid karst areas reduced soil water infiltration and evaporation, but increased transpiration. The offsetting results of these two processes may be the reason that the changes in SM content caused by vegetation restoration are so minor. In contrast, low transpiration rates in mildly humid regions owing to increased surface cover after vegetation restoration will lead to a decrease in soil evaporation and ultimately an increase in SM content (Adams et al., 1991).

Our results also demonstrated that the effects of vegetation restoration on SM content in subtropical humid karst regions exhibited seasonal differences (Fig. 10). The data indicate that the trade-off relationship between soil water infiltration and reduced evaporation and the increased transpiration caused by vegetation restoration is not uniform across seasons or different time scales. As mentioned above, the various processes appear to cancel one another out on an annual scale. However, owing to the high summer temperatures in subtropical regions, vegetation restoration increases transpiration, whereas the reductions in soil water infiltration and evaporation that result from vegetation restoration are small. This relationship also further proves that, for karst areas with surface water shortages, although vegetation restoration can improve overall soil water infiltration, the degree of improvement may be small and rates are slow.

4.2. Vegetation restoration in subtropical humid karst regions stabilizes SM

Our results show that although vegetation restoration in subtropical humid karst regions has little effect on the annual average SM content, it is beneficial for stabilizing SM (Figs. 13–15). Prior to vegetation changes, the condition of vegetation in the karst area of southwest China was poor (Chi et al., 2018), and desertification occurred over a large

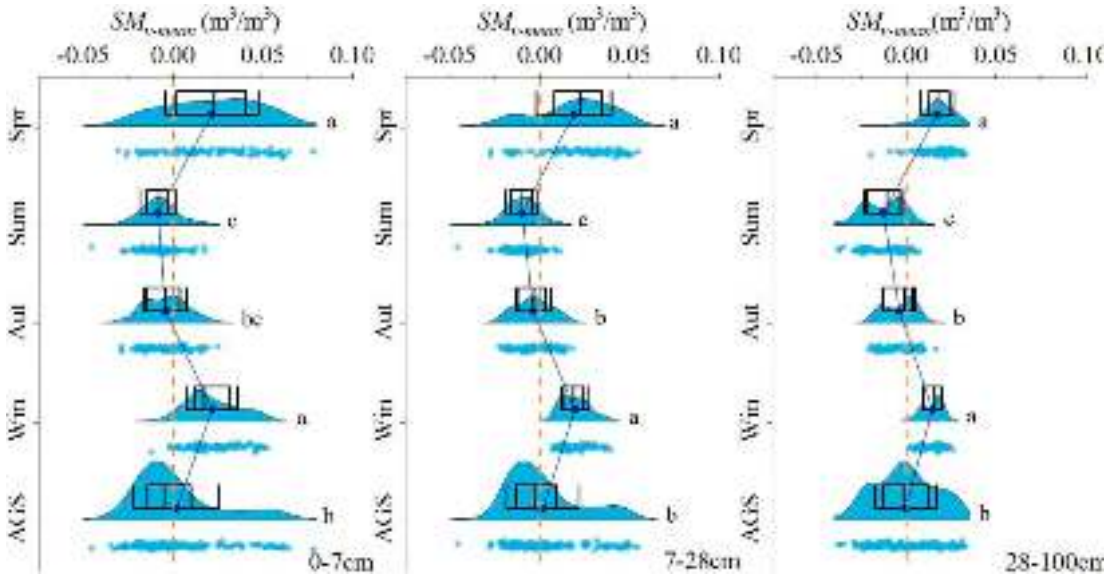

Fig. 10. Seasonal changes in average SM in different soil layers caused by vegetation restoration alone in the karst region of southwest China. Abbreviations: AGS, active growing season; Aut, autumn; Spr, spring; Sum, summer; Win, winter.

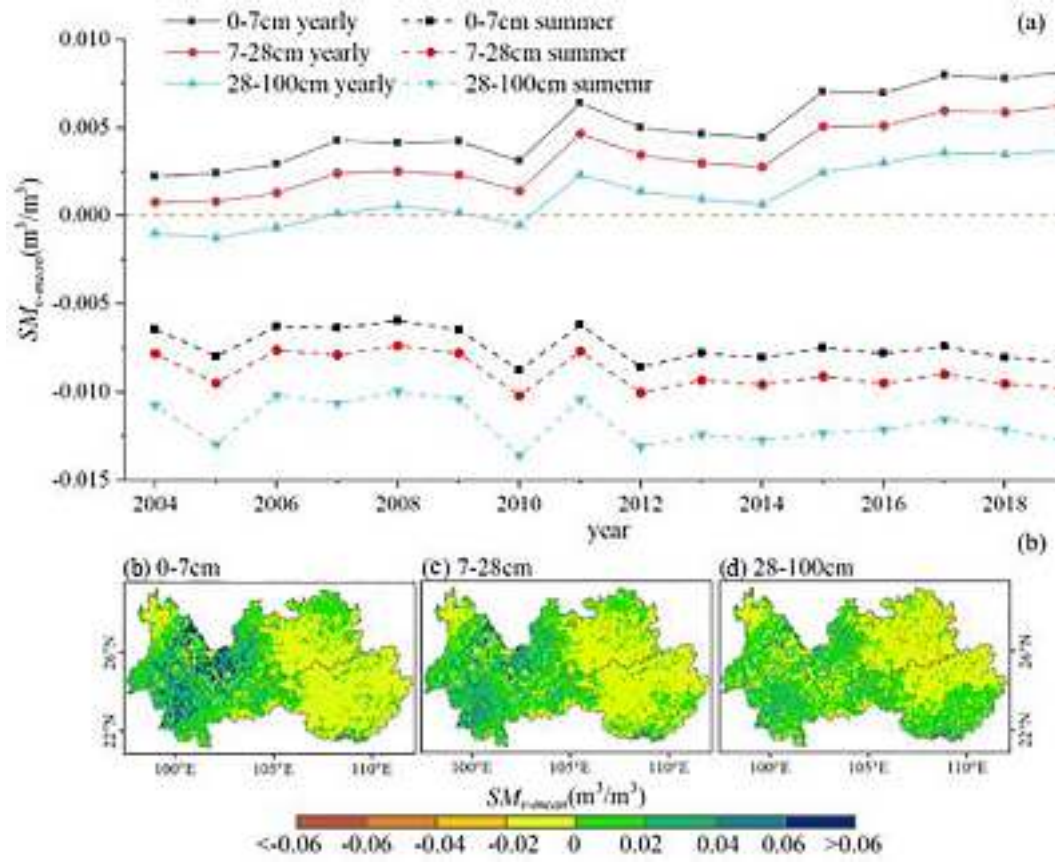

Fig. 11. The amount of annual and summer SM content change caused by vegetation restoration alone compared to before vegetation restoration (2001 as the base year) from 2014 to 2019 (a). The amount of change in SM after vegetation restoration (2019) compared with before vegetation restoration (2001) and its distribution (b,c,d).

rocky area (Fig. 17a). Coupled with the thin soil cover and high bedrock permeability in this area (Dong et al., 2019), precipitation tends to quickly either evaporate or infiltrate, making soil water storage difficult (Liu et al., 2018). This resulted in a large CV for SM prior to vegetation restoration in this area. As mentioned earlier, vegetation restoration shields the soil from the sun, which reduces evaporation. It also increases the thickness of the litter layer and changes the hydraulic properties of the soil layer, thereby increasing the water storage capacity of the litter layer and the soil layer, and reducing water seepage (Yi et al., 2021; Zhong et al., 2022) (Fig. 17b). Moreover, the greater

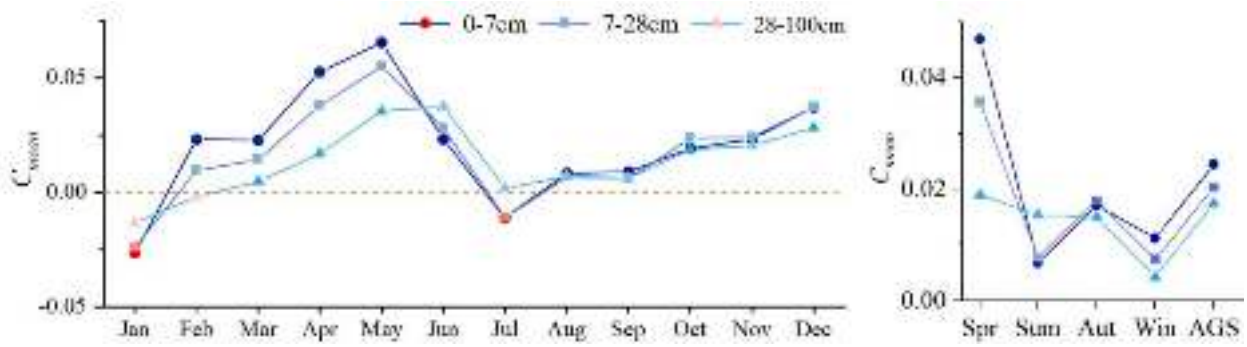

Fig. 12. Differences between changes to the average SM caused by vegetation restoration alone and the comprehensive factors. The blue symbols indicate that the average SM change caused by vegetation restoration alone is higher than the SM change caused by comprehensive factors, while the red symbols indicate the opposite.

vegetation cover can cause precipitation to be intercepted by the canopy and litter, thereby enabling longer-term replenishment of SM (Sun et al., 2022). The combined action of the above factors resulted from the restoration of vegetation in the subtropical humid karst area, resulting in greater SM stability.

Our results show that the extent of changes in SM content caused by vegetation restoration exceeds that caused by a combination of factors (including climate, vegetation restoration, and other unspecified factors) (Fig. 12). This study also shows that vegetation restoration alleviated the soil drying caused by climate warming to a certain extent. From a large-scale and long-term perspective, among the comprehensive factors that result in changes to hydrological processes, climate and vegetation restoration are the two most important (Soonthornrangsan and Lowry, 2021; Yang et al., 2022). However, precipitation in the karst areas of southwest China has essentially remained stable for the past 20 years, whereas temperature has shown a clear upward trend (Huang et al., 2021; Yang et al., 2022). These climatic changes should theoretically result in a substantial reduction in SM content. Our results show that no significant change in SM has occurred on an annual scale. This indicates that the decrease in SM content caused by rising temperatures is offset by the increase in SM content caused by vegetation restoration.

4.3. *The uniqueness of the effect of vegetation change on SM in the karst region of southwest China*

Owing to the unique karst environment, the results of this study are considerably different from those in other nonkarst vegetation restoration areas. For example, a study conducted by Qiu et al. (2021) in the Loess Plateau in north-central China showed that vegetation restoration led to a considerable reduction in SM content, which cannot be easily replenished by precipitation. However, the results of this study suggest that vegetation restoration in the karst region of southwest China mainly led to an increase in mean SM content. This difference can be attributed to the fact that the Loess Plateau is located in an arid and semiarid area, with less precipitation. Therefore, after a large-scale vegetation restoration project was conducted in this area, the SM was largely consumed by the vegetation, which greatly reduced the SM. However, the karst area of southwest China is rich in precipitation, and after vegetation restoration, the greater canopy and litter cover is able to intercept a large amount of precipitation, so that precipitation can supplement SM slowly and continuously. Therefore, vegetation restoration will not considerably reduce the mean value of SM in karst soils in southwest China.

On a long-term scale, not only vegetation will change, but climate factors, such as rainfall and temperature, will also change. Therefore, eliminating the impact of climate change is an important prerequisite for a clear understanding of the impact of vegetation restoration on SM in the karst region of southwest China. Deng et al. (2020) used SM data from 1982 to 2015 to analyze changes to SM content in karst areas. However, long-term analysis of changes to SM content could not explain the changes in SM content caused by vegetation restoration alone. Wei et al. (2021) referenced similar precipitation years to analyze changes in SM caused by vegetation restoration in the karst region of southwest China, but this study only controlled for precipitation factors and did not consider monthly and seasonal change. Temperature influences the amount of SM (Wang et al., 2018; Tang et al., 2019), but is insufficient to solely account for changes in SM caused by vegetation restoration. To address this issue, the model used in this study controlled for most environmental factors, but not vegetation. Hence, the results more accurately reflect the impact of vegetation restoration on SM in the karst region of southwest China.

4.4. *Intra-annual prediction uncertainty*

As can be seen from Fig. 6, the model in this study had a low prediction accuracy for the nongrowing season. This is mainly because only climatic and vegetation factors were considered in the RFM model in this study. This simplification achieves good prediction results in the growing season, but the relatively weaker influence of EVI during the nongrowing season means that other influencing factors on SM become more complicated, especially in the complex environmental conditions of the karst mountains (Xu et al., 2017; Gong et al., 2018; Zhou et al., 2020; Yan et al., 2022). Specifically, the ability of factors other than EVI to influence SM is relatively enhanced during the nongrowing season. These factors include temporal distribution and variability in solar radiation, wind, precipitation, air temperature, vegetation type (tree or shrub, coniferous or broad-leaved, deciduous, or not); water retention of soil and litter layers in different moisture states; hydraulic conductivity of rocks, etc. (Zhao et al., 2018; Chai et al., 2021; Lee and Kim 2022; Wei et al., 2022). However, accurate data on these factors are difficult to obtain, and there is great spatial variability in karstic mountain environments. Thus, it is difficult to fully consider all the influencing factors in the modeling stage, which is likely a common difficulty faced by most empirical models.

If certain physical process models are used, the prediction can usually be improved by parameter calibration (Baudena et al., 2008; Abdelhamed et al., 2022). However, due to the unique surface–subsurface binary nature of the hydrological system in karst environments (Liang and Yang, 1995), a large amount of surface and soil water seeps into the subsurface through dissolution fissures, and the subsurface hydrological conditions are particularly complex, so that simulating karst hydrology based on physical process models is still a major challenge (Sarrazin et al., 2018; Jeannin et al., 2021).

As mentioned earlier, there are challenges in predicting SM during nongrowing seasons in karst areas. However, if we only analyze data from growing seasons, it will not fully illustrate the overall effect of

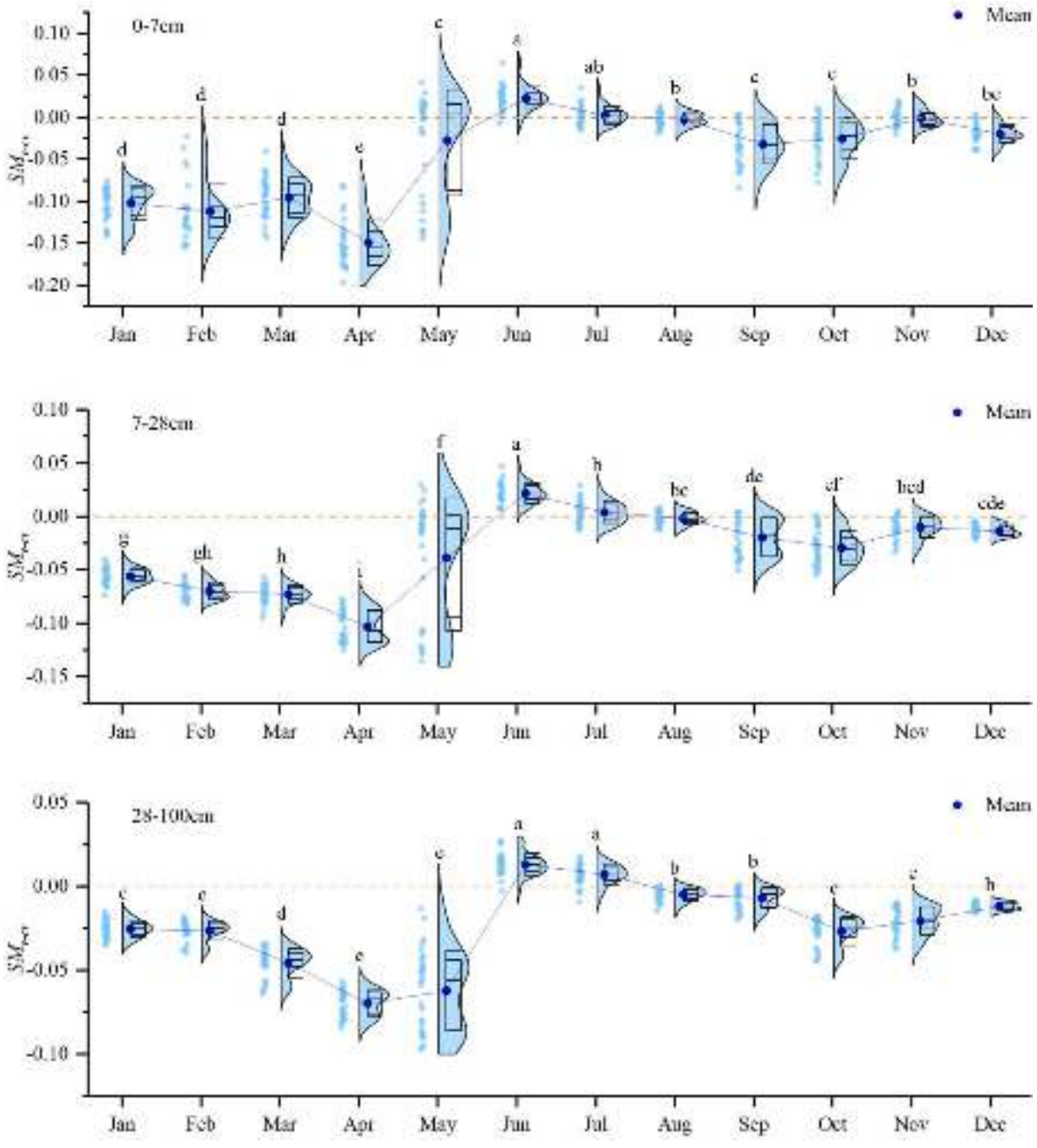

Fig. 13. Monthly changes to the CV of SM in different soil layers caused by vegetation restoration alone in the karst region of southwest China.

vegetation restoration on SM and its seasonal variation. Moreover, in humid subtropical monsoon regions like the karst region of southwest China, vegetation is not completely dormant from October to March and may still influence SM changes (Dong et al., 2022; Zhao et al., 2015). Therefore, for completeness, data from the nongrowing season were still included in the analysis. However, we recognize there is some uncertainty in the results of the nongrowing season. Therefore, we performed month-by-month, quarter-by-quarter, and growing season analyses, which not only helped show the overall results but also allowed to focus specifically on more reliable results (growing season, summer) when needed.

4.5. Limitations

The karst region of southwest China is dominated by mountains with large terrain undulations, but because of the extensive karst formations, the strong karstification complicates the environment in this area (Wei et al., 2021). The complex topography and geomorphology leads to microclimates in local areas, which strengthens spatial heterogeneity of SM. The spatial scale of all data selected in this study was 0.1° × 0.1°. Due to the large pixel range, the small spatial range cannot reflect changes to SM. Nonetheless, the SM data with this spatial resolution is presently the most reliable to date. By macro-scale analysis, such large-scale data are more conducive to reflect the overall status of SM. Therefore, although spatial resolution of the SM data is lacking, the results of this study still explain the overall spatial pattern of SM changes

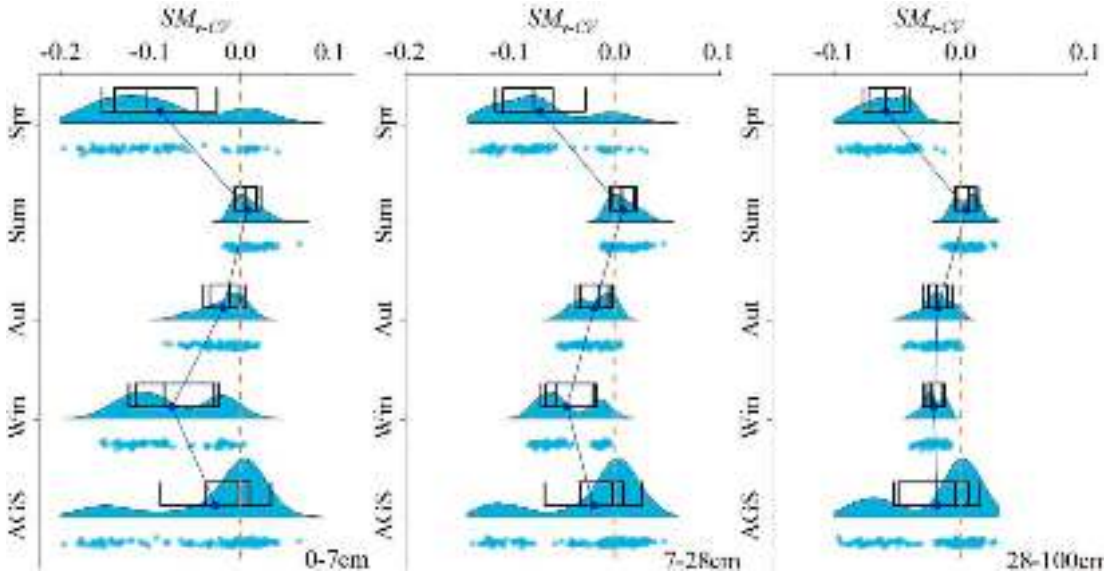

Fig. 14. Seasonal changes in the CV of SM in different soil layers caused by vegetation restoration alone in the karst region of southwest China.

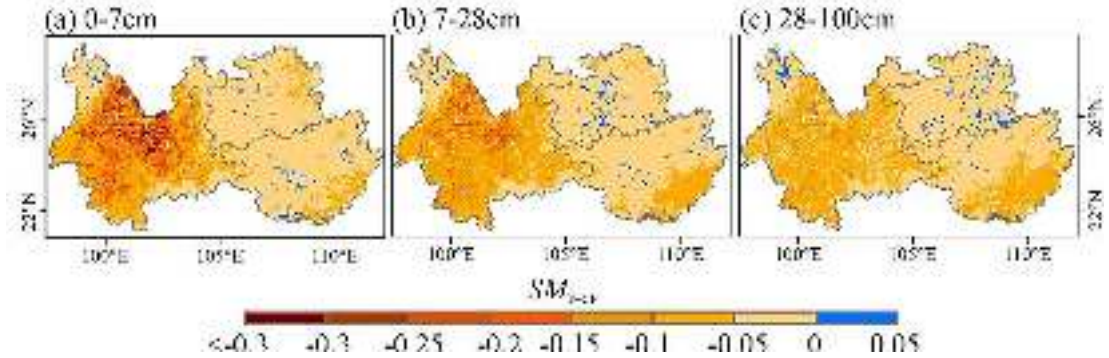

Fig. 15. Spatial distribution of the changes to the CV of SM of different soil layers on an annual scale caused by vegetation restoration alone in the karst region of southwest China.

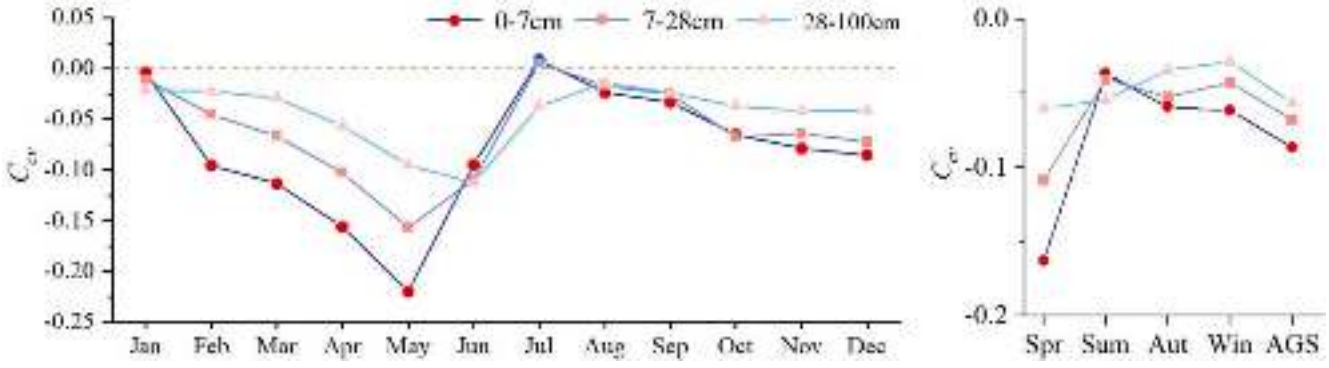

Fig. 16. Differences in changes to the CV of SM caused by vegetation restoration alone and the comprehensive factors.

caused by vegetation restoration in the karst region of southwest China.

4.6. Applications

Studies have only focused on semiarid and semi humid areas, or on humid non-karst areas. Our study based in a humid karst region provides new information for research on SM effects resulting from vegetation change. Although our results show that vegetation restoration in the karst region of southwest China has no significant effect on SM on an annual scale, the water consumption caused by vegetation restoration cannot be ignored. Our study also shows that vegetation restoration leads to a decrease in summer SM. Excessive water depletion by vegetation leads directly to reduced runoff into the river channel. This will adversely affect the availability of water resources, especially during the dry season, which cannot be ignored in the context of rapid socio-economic development and increasing water demands in these

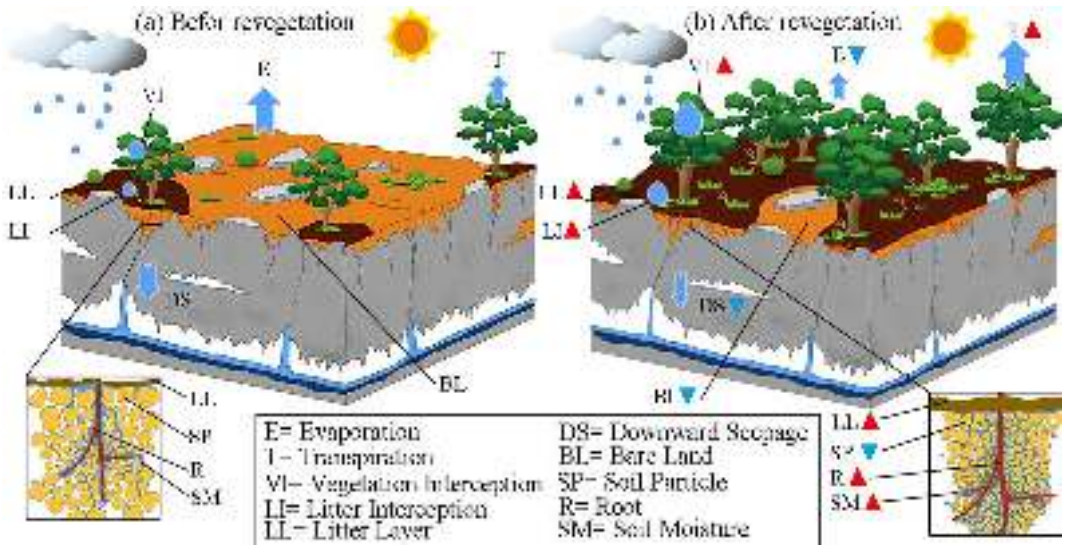

Fig. 17. Effects of changes in environmental elements caused by vegetation restoration on SM stability in subtropical humid karst regions. Red triangles in the figure represent an increase in the element, and blue triangles represent a decrease in the element.

regions. Therefore, planning for large-scale revegetation projects should strongly consider the use of low-water-consuming vegetation types to reduce the impact on water resources.

5. Conclusions

Overall, the contribution of increased vegetation to overall SM content changes in this subtropical humid karst region was 38.2 %, while the contribution of climate change was 61.8 %. Vegetation restoration in the subtropical humid karst region caused only a slight increase in SM content, although this change differed from season to season. The effect of vegetation restoration on SM changes in summer was not significant. In contrast, vegetation restoration caused a significant decrease in the variability coefficient of SM, indicating that vegetation restoration is beneficial for stabilizing SM in subtropical humid karst areas. In addition, vegetation restoration effectively moderated the drying tendency of soil caused by climate warming. The results of this work provide a more comprehensive understanding of the impact of vegetation restoration on SM in the karst region of southwest China and offer theoretical guidance for the management of ecological restoration projects in the region.

Uncited References

Chai et al. (2021), Legates et al. (2011), Segal and Xiao (2011), Soonthornrangsan and Lowry (2021), Wang and Shi (2019).

CRediT authorship contribution statement

Dawei Peng: Data curation, Writing – original draft. **Qiuwen Zhou:** Conceptualization, Funding acquisition, Project administration, Supervision, Writing – original draft. **Xin Tang:** Methodology, Software. **Weihong Yan:** Data curation, Formal analysis, Investigation. **Meng Chen:** Formal analysis, Investigation.

Declaration of Competing Interest

The authors declare that they have no known competing financial interests or personal relationships that could have appeared to influence the work reported in this paper.

Data availability

Data will be made available on request.

Acknowledgments

This work was supported by the Scientific and Technological Research Project of Guizhou Province [grant number Qiankehe Jichu [2019]1433 & Qiankehe Pingtai Rencai [2017]5726], the National Science Foundation of China [grant number 41761003 & 41801293], the Joint Fund of the National Natural Science Foundation of China and the Karst Science Research Center of Guizhou Province [grant number U1812401], the Foundation Programme for Outstanding Talents in Higher Education Institutions of Guizhou Province [grant number [2018]042].

References

Abdelhamed, M.S., Elshamy, M.E., Wheater, H.S., et al., 2022. Hydrologic-land surface modelling of the Canadian sporadic-discontinuous permafrost: initialization and uncertainty propagation. Hydrol. Process. 36 (3), e14509.
Adams, P.W., Flint, A.L., Fredriksen, R.L., 1991. Long-term patterns in soil moisture and revegetation after a clearcut of a Douglas-fir forest in Oregon. For. Ecol. Manage. 41 (3–4), 249–263.
Albergel, C., De Rosnay, P., Gruhier, C., et al., 2012. Evaluation of remotely sensed and modelled soil moisture products using global ground-based in situ observations. Remote Sens. Environ. 118, 215–226.
Baudena, M., d'Andrea, F., Provenzale, A., 2008. A model for soil-vegetation-atmosphere interactions in water-limited ecosystems. Water Resour. Res. 44 (12).
Bellot, J., Maestre, F.T., Chirino, E., et al., 2004. Afforestation with Pinus halepensis reduces native shrub performance in a Mediterranean semiarid area. Acta Oecologica 25 (1–2), 7–15.
Breiman, L., 2001. Random forests. Machine Learning 45 (1), 5–32.
Brocca, L., Melone, F., Moramarco, T., et al., 2010. Improving runoff prediction through the assimilation of the ASCAT soil moisture product. Hydrol. Earth Syst. Sci. 14 (10), 1881–1893.
Cámara, J., Gómez-Miguel, V., Martín, M.Á., 2017. Lithologic control on soil texture heterogeneity. Geoderma 287, 157–163.
Cao, J., Tian, H., Adamowski, J.F., et al., 2018. Influences of afforestation policies on soil moisture content in China's arid and semi-arid regions. Land Use Policy 75, 449–458.
Carranza, C., Nolet, C., Pezij, M., et al., 2021. Root zone soil moisture estimation with Random Forest. J. Hydrol. 593, 125840.
Chai, Q., Wang, T., Di, C., 2021. Evaluating the impacts of environmental factors on soil moisture temporal dynamics at different time scales. J. Water Clim. Change 12 (2), 420–432.
Chi, D., Wang, H., Li, X., et al., 2018. Estimation of the ecological water requirement for natural vegetation in the Ergune River basin in Northeastern China from 2001 to 2014. Ecol. Ind. 92, 141–150.

Deng, Y., Wang, S., Bai, X., et al., 2020. Spatiotemporal dynamics of soil moisture in the karst areas of China based on reanalysis and observations data. J. Hydrol. 585, 124744.
Dong, X., Cohen, M.J., Martin, J.B., et al., 2019. Ecohydrologic processes and soil thickness feedbacks control limestone-weathering rates in a karst landscape. Chem. Geol. 527, 118774.
Dong, B., Yu, Y., Pereira, P., 2022. Non-growing season drought legacy effects on vegetation growth in southwestern China. Sci. Total Environ., 157334
Feng, H., 2016. Individual contributions of climate and vegetation change to soil moisture trends across multiple spatial scales. Sci. Rep. 6, 32782.
Feng, H., Liu, Y., 2015. Combined effects of precipitation and air temperature on soil moisture in different land covers in a humid basin. J. Hydrol. 531, 1129–1140.
Fu, Z.Y., Chen, H.S., Zhang, W., et al., 2015. Subsurface flow in a soil-mantled subtropical dolomite karst slope: a field rainfall simulation study. Geomorphology 250, 1–14.
Fu, T., Chen, H., Fu, Z., et al., 2016. Surface soil water content and its controlling factors in a small karst catchment. Environ. Earth Sci. 75 (21), 1–11.
Gong, Y., Tian, R., Li, H., 2018. Coupling effects of surface charges, adsorbed counterions and particle-size distribution on soil water infiltration and transport. Eur. J. Soil Sci. 69 (6), 1008–1017.
Gu, X., Zhang, Q., Li, J., et al., 2019. Attribution of global soil moisture drying to human activities: a quantitative viewpoint. Geophys. Res. Lett. 46 (5), 2573–2582.
Hartmann, A., Goldscheider, N., Wagener, T., et al., 2014. Karst water resources in a changing world: review of hydrological modeling approaches. Rev. Geophys. 52 (3), 218–242.
Heathman, G.C., Starks, P.J., Ahuja, L.R., et al., 2003. Assimilation of surface soil moisture to estimate profile soil water content. J. Hydrol. 279 (1–4), 1–17.
Hiltbrunner, D., Zimmermann, S., Karbin, S., et al., 2012. Increasing soil methane sink along a 120-year afforestation chronosequence is driven by soil moisture. Glob. Change Biol. 18 (12), 3664–3671.
Huang, J., Ge, Z., Huang, Y., et al., 2021. Climate change and ecological engineering jointly induced vegetation greening in global karst regions from 2001 to 2020. Plant Soil 1–20.
Huang, Y., Zhao, P., Zhang, Z., et al., 2009. Transpiration of Cyclobalanopsis glauca (syn. Quercus glauca) stand measured by sap-flow method in a karst rocky terrain during dry season. Ecol. Res. 24 (4), 791–801.
Jeannin, P.Y., Artigue, G., Butscher, C., et al., 2021. Karst modelling challenge 1: results of hydrological modelling. J. Hydrol. 600, 126508.
Lee, E., Kim, S., 2022. Spatiotemporal soil moisture response and controlling factors along a hillslope[J]. J. Hydrol. 605, 127382.
Legates, D.R., Mahmood, R., Levia, D.F., et al., 2011. Soil moisture: a central and unifying theme in physical geography. Prog. Phys. Geogr. 35 (1), 65–86.
Li, Z., Xu, X., Xu, C., et al., 2017. Annual runoff is highly linked to precipitation extremes in karst catchments of southwest China. J. Hydrometeorol. 18 (10), 2745–2759.
Li, X., Xu, X., Liu, W., et al., 2019. Revealing the scale-specific influence of meteorological controls on soil water content in a karst depression using wavelet coherency. Agric. Ecosyst. Environ. 279, 89–99.
Liang, H., Yang, M.D., 1995. Analysis of confluence processes in karst basin hydrogeomorphic system-a case study of karst crest depression valley basin. Carsologica Sinica 14 (02), 186–193. In Chinese.
Liang, H., Xue, Y., Li, Z., et al., 2018. Soil moisture decline following the plantation of Robinia pseudoacacia forests: Evidence from the Loess Plateau. For. Ecol. Manage. 412, 62–69.
Liu, Y., Miao, H.T., Huang, Z., et al., 2018. Soil water depletion patterns of artificial forest species and ages on the Loess Plateau (China). For. Ecol. Manage. 417, 137–143.
Mittelbach, H., Seneviratne, S.I., 2012. A new perspective on the spatio-temporal variability of soil moisture: temporal dynamics versus time-invariant contributions. Hydrol. Earth Syst. Sci. 16 (7), 2169–2179.
Niether, W., Schneidewind, U., Armengot, L., et al., 2017. Spatial-temporal soil moisture dynamics under different cocoa production systems. Catena 158, 340–349.
Ning, T., Liu, W., Li, Z., et al., 2020. Modelling and attributing evapotranspiration changes on China's Loess Plateau with Budyko framework considering vegetation dynamics and climate seasonality. Stoch. Environ. Res. Risk Assess. 34 (8), 1217–1230.
Qiu, L., et al., 2021. Quantifying spatiotemporal variations in soil moisture driven by vegetation restoration on the Loess Plateau of China. J. Hydrol. 600, 126580.
Sarrazin, F., Hartmann, A., Pianosi, F., et al., 2018. V2Karst V1. 1: a parsimonious large-scale integrated vegetation–recharge model to simulate the impact of climate and land cover change in karst regions. Geosci. Model Dev. 11 (12), 4933–4964.
Segal, M., Xiao, Y., 2011. Multivariate random forests. Wiley Interdiscip. Rev.: Data Min. Knowl. Discov. 1 (1), 80–87.
Soonthornrangsan, J.T., Lowry, C.S., 2021. Vulnerability of water resources under a changing climate and human activity in the lower Great Lakes region. Hydrol. Process. 35 (12), e14440.
Sun, S., Xiang, W., Ouyang, S., et al., 2022. Higher canopy interception capacity of forests restored to the climax stage in subtropical China. Hydrol. Process. 36 (3), e14538.
Tang, M., Zhao, X., Gao, X., et al., 2019. Land use affects soil moisture response to dramatic short-term rainfall events in a hillslope catchment of the Chinese Loess Plateau. Agron. J. 111 (3), 1506–1515.
Van Hall, R.L., Cammeraat, L.H., Keesstra, S.D., et al., 2017. Impact of secondary vegetation succession on soil quality in a humid Mediterranean landscape. Catena 149, 836–843.
Wang, Q., Shan, J., Jiaqi, Z., et al., 2022. Effects of vegetation restoration on evapotranspiration water consumption in mountainous areas and assessment of its remaining restoration space. J. Hydrol. 605, 127259.
Wang, A., Shi, X., 2019. A multilayer soil moisture dataset based on the gravimetric method in China and its characteristics. J. Hydrometeorl. 20, 1721–1736.
Wang, Y., Yang, J., Chen, Y., et al., 2018. The spatiotemporal response of soil moisture to precipitation and temperature changes in an arid region, China. Remote Sens. 10 (3), 468.
Wei, X., Zhou, Q., Cai, M., et al., 2021. Effects of vegetation restoration on regional soil moisture content in the humid karst areas—a case study of Southwest China. Water 13 (3), 321.
Wei, X., Gao, J., Liu, S., et al., 2022. Temporal variation of soil moisture and its influencing factors in karst areas of Southwest China from 1982 to 2015. Water 14 (14), 2185.
Xu, G., Zhang, T., Li, Z., et al., 2017. Temporal and spatial characteristics of soil water content in diverse soil layers on land terraces of the Loess Plateau, China. Catena 158, 20–29.
Yan, W., Zhou, Q., Peng, D., et al., 2021. Soil moisture responses under different vegetation types to winter rainfall events in a humid karst region. Environ. Sci. Pollut. Res. 28 (40), 56984–56995.
Yan, W., Zhou, Q., Peng, D., et al., 2022. Response of surface-soil quality to secondary succession in karst areas in Southwest China: case study on a limestone slope. Ecol. Eng. 178, 106581.
Yang, H., Hu, J., Zhang, S., et al., 2022. Climate variations vs. human activities: distinguishing the relative roles on vegetation dynamics in the Three Karst Provinces of Southwest China. Front. Earth Sci. 10, 799493.
Yang, L., Wei, W., Chen, L., et al., 2014. Response of temporal variation of soil moisture to vegetation restoration in semi-arid Loess Plateau, China. Catena 115, 123–133.
Yang, J., Xu, X., Liu, M., et al., 2016. Effects of Napier grass management on soil hydrologic functions in a karst landscape, southwestern China. Soil Tillage Res. 157, 83–92.
Yang, J., Xu, X., Liu, M., et al., 2017. Effects of "Grain for Green" program on soil hydrologic functions in karst landscapes, southwestern China. Agric. Ecosyst. Environ. 247, 120–129.
Yi, R., Xu, X., Zhu, S., et al., 2021. Difference in hydraulic resistance between planted forest and naturally regenerated forest and its implications for ecosystem restoration in subtropical karst landscapes. J. Hydrol. 596, 126093.
Yu, X.N., Huang, Y.M., Li, E.G., et al., 2018. Effects of rainfall and vegetation to soil water input and output processes in the Mu Us Sandy Land, northwest China. Catena 161, 96–103.
Yu, B., Liu, G., Liu, Q., 2020. Effects of land use changes for ecological restoration on soil moisture on the Chinese Loess Plateau: a meta-analytical approach. J. For. Res. 31 (2), 443–452.
Zhang, Z., Chen, X., Huang, Y., et al., 2014. Effect of catchment properties on runoff coefficient in a karst area of southwest China. Hydrol. Process. 28 (11), 3691–3702.
Zhang, Y., Shangguan, Z., 2016. The coupling interaction of soil water and organic carbon storage in the long vegetation restoration on the Loess Plateau. Ecol. Eng. 91, 574–581.
Zhang, Y., Deng, L., Yan, W., et al., 2016. Interaction of soil water storage dynamics and long-term natural vegetation succession on the Loess Plateau, China. Catena 137, 52–60.
Zhang, Y., Xu, X., Li, Z., et al., 2019. Effects of vegetation restoration on soil quality in degraded karst landscapes of southwest China. Sci. Total Environ. 650, 2657–2665.
Zhang, L., Zeng, Y., Zhuang, R., et al., 2021. In situ observation-constrained global surface soil moisture using random forest model. Remote Sens. 13 (23), 4893.
Zhang, X., Zhang, G., Hu, C., et al., 2020. Response of soil moisture to landscape restoration in the hilly and gully region of the Loess Plateau, China. Biologia 75 (6), 827–839.
Zhao, W., Fang, X., Daryanto, D., et al., 2018. Factors influencing soil moisture in the Loess Plateau, China: a review. Earth Environ. Sci. Trans. Royal Soc. Edinburgh 109 (3–4), 501–509.
Zhao, X., Wei, H., Liang, S., et al., 2015. Responses of natural vegetation to different stages of extreme drought during 2009–2010 in Southwestern China. Remote Sens. 7 (10), 14039–14054.
Zhong, F., Xu, X., Li, Z., et al., 2022. Relationships between lithology, topography, soil, and vegetation, and their implications for karst vegetation restoration. Catena 209, 105831.
Zhou, L., Wang, X., Wang, Z., et al., 2020. The challenge of soil loss control and vegetation restoration in the karst area of southwestern China. Int. Soil Water Conserv. Res. 8 (1), 26–34.
Zhou, Q., Zhu, A., Yan, W., et al., 2022. Impacts of forestland vegetation restoration on soil moisture content in humid karst region: a case study on a limestone slope. Ecol. Eng. 180, 106648.